



**HAL**  
open science

## **Verticillium Wilt on Fiber Flax: Symptoms and Pathogen Development In Planta**

Adrien Blum, Melanie Bressan, Abderrakib Zahid, Isabelle Trinsoutrot-Gattin, Azeddine Driouich, Karine Laval

### ► To cite this version:

Adrien Blum, Melanie Bressan, Abderrakib Zahid, Isabelle Trinsoutrot-Gattin, Azeddine Driouich, et al.. Verticillium Wilt on Fiber Flax: Symptoms and Pathogen Development In Planta. Plant Disease, 2018, 102 (12), pp.2421-2429. 10.1094/PDIS-01-18-0139-RE . hal-01963019

**HAL Id: hal-01963019**

**<https://normandie-univ.hal.science/hal-01963019>**

Submitted on 31 May 2021

**HAL** is a multi-disciplinary open access archive for the deposit and dissemination of scientific research documents, whether they are published or not. The documents may come from teaching and research institutions in France or abroad, or from public or private research centers.

L'archive ouverte pluridisciplinaire **HAL**, est destinée au dépôt et à la diffusion de documents scientifiques de niveau recherche, publiés ou non, émanant des établissements d'enseignement et de recherche français ou étrangers, des laboratoires publics ou privés.



25 the development of hyphae on root epidermis more particularly on zone of cell differentiation  
26 and around emerging lateral roots while the zone of cell division and the root tip were free of  
27 the pathogen. At three days post inoculation, the zone of cell differentiation and lateral roots  
28 were embedded into a fungal mass. Swelling structures such as appressoria, were observed at  
29 one week post inoculation. At two weeks post inoculation and onwards, the pathogen had  
30 colonized xylem vessels in roots, followed by the stem and finally leaves during the  
31 symptomatic stage. Additionally, observations of infected plants after retting in field revealed  
32 microsclerotia embedded inside the bast fiber bundle, thus contributing, potentially to  
33 weakening of fiber. All of these results provide a global account of the *V. dahliae*  
34 development when infecting fiber flax.

## 35 **Introduction**

36 Fiber flax (*Linum usitatissimum* L.) is an important source of fiber used for textile  
37 manufacture and composite materials (van Sumere, 1992). Currently, France is the worldwide  
38 leader in fiber flax production, ahead of Belgium, Belarus and Russian federation (FAOSTAT  
39 data 2016); more than half of this production is grown in the Normandy region  
40 (<http://www.chambre-agriculture-normandie.fr/panorama-lin-normandie/>). Historically, most  
41 research on flax diseases has focused on Fusarium wilt (caused by *Fusarium oxysporum* f.sp.  
42 *lini*) and rust (caused by *Melampsora lini*) which have been the main limiting factors in flax  
43 production (Rashid, 2003). However, among other harmful flax diseases, Verticillium wilt, a  
44 vascular disease caused by the soil borne fungus *Verticillium dahliae* Kleb. is becoming  
45 increasingly prevalent among fiber flax culture in France (Valade *et al.*, 2015;  
46 <http://www.fiches.arvalis-infos.fr/>).

47 Verticillium wilt is caused by species of the group *Verticillium sensu stricto* (Klosterman *et*  
48 *al.*, 2009) and constitutes a major threat to a broad range of crop, leading to significant yield  
49 losses (Agrios, 1997; Pegg and Brady, 2002). Among the *Verticillium* species, *V. dahliae* has  
50 the largest host range (Inderbitzin and Subbarao, 2014) and the most significant economic  
51 impact, causing billion dollars losses worldwide (Pegg and Brady, 2002). The pathogen can  
52 form black pigmented, multicellular resting structures, so-called, microsclerotia that can  
53 remain viable in the soil or in debris for 20 years (Wilhelm, 1955; Devay *et al.*, 1974; Krikun  
54 *et al.*, 1990). Verticillium wilt is difficult to control because of its inaccessibility during  
55 infection, long-term persistence in fields, broad host range and scarcity of resistant plants. At  
56 present, no efficient solution exists, even if research on varietal selection, agronomic methods  
57 and antagonist microbes seems to be promising (Fradin and Thomma, 2006; Klosterman *et*  
58 *al.*, 2009; Yadeta and Thomma, 2013). Several studies focused on race-specific resistance  
59 have highlighted an allelic form of *Vel*, a gene encoding a cell-surface glycoprotein that leads

60 to an incompatible reaction with *V. dahliae* race 1 pathotypes. *V. dahliae* race 1 strains are  
61 more aggressive than so-called race 2 strains on susceptible tomato cultivars (Schaible *et al.*,  
62 1951; Rick *et al.*, 1959; Grogan *et al.*, 1979; Diwan *et al.*, 1999; Kawchuk *et al.* 2001; Fradin  
63 *et al.*, 2009; de Jonge *et al.*, 2012). To date, there is no fiber flax variety resistant to *V. dahliae*  
64 and no effective chemical control. In addition, the six-seven year interval between two flax  
65 cultures in crop rotation recommended to fight against soil-borne diseases is limited because  
66 the inoculum is present for up to 20 years in soil and could have a broad host range.  
67 Therefore, the understanding of the pathogen infection, colonization and subsequent  
68 symptoms produced on fiber flax must be the first step towards innovative solutions against  
69 this disease.

70 On various plants, infection by *V. dahliae* occurs at the root surface level, fungal hyphae later  
71 invade xylem vessels and progress slowly in acropetal direction, i.e. from the bottom to top of  
72 the plant. Upon germination, each microsclerotium has the capacity to produce one to several  
73 infection hyphae thus increasing the chance to engender a successful infection (Fitzell *et al.*,  
74 1980). However few of the infections lead to xylem colonization: Gerik and Huisman (1988)  
75 have estimated that 0.02% of root infections lead to systemic colonization in cotton.  
76 Similarly, when eggplant roots were inoculated with *V. dahliae* microsclerotia only 1 out of  
77 205 infections led to systemic colonization (Bejarano-Alcazar *et al.*, 1999). Recent studies of  
78 *V. dahliae* on different hosts were carried out by green fluorescent protein (GFP) transformed  
79 strains (inoculum of conidia) and confocal laser scanning microscopy (CLSM), therefore  
80 providing substantial knowledge about the infection process on root and the colonization  
81 within the plant (Vallad and Subbarao, 2008; Zhang *et al.*, 2012; Maruthachalam *et al.* 2013;  
82 Zhao *et al.*, 2014). According to these studies, germination of conidia on inoculated plants  
83 was generally fast, in less than 24 hours one germ tube emerged from one or both ends of a  
84 conidium. Thereafter, the germinated conidia developed rapidly appressoria or evolved in a

85 complex hyphal network that formed later appressoria between junctions of epidermal cells,  
86 points of entry for the further internal colonization (Vallad and Subbarao, 2008). On  
87 *Arabidopsis*, spinach or lettuce, hyphae growth followed the longitudinal axis of epidermal  
88 cells and was generally intercellular (Vallad and Subbarao, 2008; Maruthachalam *et al.* 2013;  
89 Zhao *et al.*, 2014). However, even if the infection occurs rapidly, the preferential root zones  
90 leading to a successful one vary according to the reports. For example, substantial  
91 colonization was limited to the tip of lateral roots and within the root elongation zone on  
92 lettuce (Vallad and Subbarao, 2008). On *Arabidopsis*, only the root hair zone was colonized  
93 by germinated conidia (Zhao *et al.*, 2014). In contrast, Zhang *et al.*, (2012) observed that most  
94 of conidia were on the meristematic and the elongation zones of cotton roots, but rarely on the  
95 root cap and none on the root hair. On spinach root, vascular colonization started from the  
96 root tip, in addition, a complex hyphal network leading to later infections was observed on the  
97 surface of the elongation zone (Maruthachalam *et al.* 2013). Internal colonization started  
98 within the elongation zone by entering the root cortical tissue intra-intercellularly,  
99 subsequently the pathogen hyphae reached the xylem vessels (Vallad and Subbarao, 2008;  
100 Maruthachalam *et al.* 2013; Zhao *et al.*, 2014). Once vascular colonization established, the  
101 hyphae colonized neighboring vessels via pit pairs or perforation plates and the pathogen  
102 development slowly extended to the lateral roots (Vallad and Subbarao, 2008). The pathogen  
103 was either restricted to individual vessels (cotton or lettuce) or all of the xylem vessels are  
104 densely colonized (spinach). The hyphae progressed acropetally through root vessels towards  
105 the above-ground parts together with conidia production, accelerating the colonization by  
106 moving rapidly with the transpiration stream. Ultimately, the pathogen was also detected in  
107 upper stem, inflorescence and seed, leading to further contamination to the developing  
108 seedlings (Vallad and Subbarao, 2008; Maruthachalam *et al.* 2013; Zhao *et al.*, 2014).

109 Only a few scientific reports have dealt with *Verticillium* wilt on flax, Marchal (1940) reports  
110 wilting symptoms on plants and the presence of microsclerotia on roots in Belgium;  
111 Hoffmann and Rondonanski (1959) mention that *Verticillium* wilt is responsible for fiber that  
112 is brittle and consequently non-marketable; Fitt *et al.*, (1992) describe *Verticillium* wilt  
113 symptoms and assess its occurrence and severity in some UK and German fields. According  
114 to the French monitoring organizations, symptoms on fiber flax related to *Verticillium* wilt  
115 have a metallic blue appearance on stems during retting (process employing the action of  
116 microorganisms to separate fiber from the other parts of the plant) that become brittle and  
117 fragile, thus causing damage. The damage causes considerable yield losses, and depreciated  
118 fibers are consequently difficult to upgrade. However, before retting, *Verticillium* wilt is  
119 hardly diagnosable because of possible confusion with water stress or *Fusarium* wilt (Valade  
120 *et al.*, 2015; <http://www.fiches.arvalis-infos.fr/>). On various plants affected with *Verticillium*  
121 wilt, necrotic lesions at the root cap or vascular discolorations within the root in advance of  
122 the pathogen colonization may be the first symptoms to be observed (Eastburn and Chang,  
123 1994; Vallad *et al.* 2006; Vallad and Subbarao, 2008). Leaves wilting are triggered a few  
124 weeks after inoculation usually in the oldest shoots, wilting starts at one half of an infected  
125 leaf and slowly progress acropetally. Plants affected with *Verticillium* wilt are usually stunted  
126 and their vascular tissues show characteristic brownish discoloration. Defoliation, gradual  
127 wilting and death of successive branches, or the abrupt collapse and death of the entire plant,  
128 may all be consequences of *Verticillium* wilt (Agrios, 2005). However, the consequence of a  
129 *Verticillium* infection can be different between hosts; there are no unique symptoms that exist  
130 in all plants (Fradin and Thomma, 2006). For example, infection on tomato triggers  
131 yellowing, and necrosis of the tips and edges of lower leaves, causing typical V-shaped  
132 lesions. In some cases, the veins may turn purple or brown, and yellow blotches may appear  
133 on leaves that later become necrotic and brown (Fradin and Thomma, 2006). Wilt symptoms

134 on spinach first affect bolting stem, then inflorescence including bracts that develop a  
135 chlorosis and flaccid aspect (Maruthachalam *et al.* 2013). On lettuce, *Verticillium* wilt  
136 symptoms first consists of angular chlorosis regions on leaves that become flaccid, then  
137 evolving into angular areas of necrosis (Pegg and Brady, 2002; Vallad *et al.* 2006).

138 Considering that the symptoms and the resulting damage is unique in each host plant-*V.*  
139 *dahliae* interactions and the lack of reports on *Verticillium* wilt on fiber flax, we provide a  
140 complete description of observed symptoms and of the pathogen development, including  
141 spatial and temporal pathogen progress on the root, stem and leaf, as monitored by CLSM.

## 142 **Materials and methods**

### 143 **Plant material**

144 Fiber flax seeds (*Linum usitatissimum* L.) cv. Adélie were provided by the cooperative Terre  
145 de Lin (Saint-Pierre-le-Vigier, France). Seeds were sterilized by immersion in 70% ethanol  
146 for 2 min, rinsed in sterile water for 5 min, immersed in sodium hypochlorite 2.6% (v/v) for  
147 10 min and finally rinsed three times in sterile water before sowing. In July 2014, a 12.5  
148 hectare fiber flax plot (*Linum usitatissimum* L., cv. Aretha) was investigated in La Haye  
149 Aubrée, France (49°39'73.0" N; 0°67'50.1" E) approximately 3 months after planting  
150 (capsule stage). Within the plot, an infectious site containing wilting plants was clearly  
151 visible, thus susceptible to be affected by *Verticillium* wilt. Twenty samples of infected plants  
152 (C1 to C20) and 20 of non-infected were collected (Fig. 7A). Samples of flax straws, brittle or  
153 not were collected in September 2014 (post retting) from the same plot.

### 154 **Pathogen strains**

155 The *V. dahliae* strain VdLu01 was previously sampled from straw of diseased fiber flax during  
156 retting on August 2005 in Gueures (Upper Normandy, France) by Terre de Lin. This strain

157 has the capacity to produce enough inoculum for an experimental assay. The department of  
158 Plant Pathology (University of California, Davis, CA USA) provided *V. dahliae* strains  
159 VdLs16 and VdLs17, isolated on lettuce and previously described as race 1 and race 2,  
160 respectively (Vallad *et al.*, 2006), both of which were transformed with the GFP gene.  
161 Fluorescence was checked using an epi fluorescent microscope (DM1000, Leica, Germany)  
162 fitted with a 50 W Hg lamp (Leica, Germany). To obtain pathogen inoculum, each strain was  
163 grown in potato dextrose broth (PDA - 26.5 g.l<sup>-1</sup>) with sterile water in 500 ml Erlenmeyer  
164 flask, placed on an agitator (150 rpm) for fifteen days at 20°C in the dark. Conidia were  
165 subsequently isolated in PBS (phosphate buffered saline) by crushing fungal masse on a 100  
166 µm pore sieve. Recovered conidia were counted on a Malassez cell and adjusted to 10<sup>6</sup>  
167 conidia per mL before inoculation. Microsclerotia were obtained by using malt extract (MA -  
168 10 g.l<sup>-1</sup>) with sterile water in 500 ml Erlenmeyer flask for one month at 20°C in the dark.

### 169 **Inoculation procedure and plants cultivation**

170 Two systems, a hydroponic/root-dipping method and a peat system/soil-drench method, were  
171 used for plant cultivation and inoculation. In both systems plants were inoculated with  
172 VdLu01 and VdLs17 at a concentration of 10<sup>6</sup> conidia per mL. All experiments were  
173 performed in a growth chamber at 23°C, with a 16h light and 8h dark photoperiod. The  
174 hydroponic/root-dipping method was used for symptomatic observations and CLSM analysis  
175 (roots and above-ground parts). Sterilized seeds were sowed in sterile Murashige & Skoog  
176 medium (4.3 g.L<sup>-1</sup>) solidified with agar (15 g.L<sup>-1</sup>). Ten-day seedlings were gently sampled.  
177 Roots were immersed for 1 hour in a conidia solution or in PBS as a control. The root  
178 seedlings were subsequently transferred into sterile hydroponic Hoagland medium (Hoagland  
179 and Arnon, 1950). The peat system/soil-drench method was used for symptomatic  
180 observations and CLSM analysis (above-ground parts). Sterilized seeds were sowed in Jiffy-  
181 7® pots (Jiffy Products International BV, Moerdijk, The Netherlands) with 1 seed per pot.

182 The bottom of the Jiffy pots containing ten days seedlings were drenched 1 hour into conidia  
183 solution or in PBS for controls. Jiffy pots were next transplanted into larger peat pots and  
184 plant stakes were set up after 3 weeks.

### 185 **Light microscopy**

186 Plant symptoms were imaged on a digital microscope (VHX-5000, Keyence, Japan) with VH-  
187 Z20R and VH-Z100R (fitted with an OP-72405 polarization illumination attachment)  
188 objectives (Keyence, Japan) and *V. dahliae* fungal structures were imaged on a transmitted  
189 light microscope (DM1000, Leica, Germany) with x10 and x100 objectives at UniLaSalle  
190 (Mont-Saint-Aignan, France). Fresh and fixed samples in methanol (according to Zelko *et al.*,  
191 2012) were observed. Cross sections of stems and roots were hand-cut under a binocular  
192 microscope then mounted on a glass slide with glycerol 80% (v/v). Lactophenol blue solution  
193 (Sigma Aldrich, Saint Louis MO, USA) was used to stain fungal structure. Briefly, mycelium  
194 was stained 5 min on glass slide then rinsed with distilled water before observation.

### 195 **Confocal laser scanning microscopy (CLSM)**

196 Samples were fixed in methanol and then stored at 4°C as described Zelko *et al.*, 2012 for  
197 further analyses. Root samples were sectioned because of their large size and longitudinal and  
198 cross sections of stems were hand-cut under a binocular microscope. All samples were  
199 mounted on a glass slide with distilled water. Images were acquired by CLSM (TCS SP2  
200 AOBS and TCS SP8 MP, Leica, Germany) at Primacén, Mont-Saint-Aignan France.  
201 Observations were performed using x10, x25, x40 and x100 oil immersion objectives. GFP  
202 fluorescence was detected by a 488-nm ray line of an argon laser and emissions were  
203 collected in the range of 498 and 570 nm. Fluorescent and transmitted light captures were  
204 performed then; overlay images and scales were obtained by ImageJ software (Rasband WS,  
205 1997-2015, <http://imagej.nih.gov/ij/>, 1997-2015).

**206 Plant and fungal DNA extraction and quantification**

207 Up to 50 mg of plant (stem or straw, non-infected or infected) or fungus (pure culture)  
208 samples were transferred to -20°C before use. Plant samples were previously finely cut before  
209 DNA extraction. Total DNA extraction was performed using a PowerPlant DNA Isolation kit  
210 (MoBio Laboratories, Carlsbad CA, USA) following the manufacturer's instructions.  
211 Concerning fungal samples, a preliminary step were added. Fungal tissues were crushed with  
212 a sterile pestle and subsequently digested at 30°C overnight in 450 µL of PowerPlant bead  
213 solution with the addition of 400 U of a lyticase solution (Sigma Aldrich, Saint Louis MO,  
214 USA). Total DNA concentrations were assessed using a Fluorescent DNA quantification kit  
215 (Bio-Rad, Hercules CA, USA) and a Varioskan™ Flash Multimode Reader  
216 (ThermoScientific, Waltham MA, USA) following manufacturer's instructions. All extracted  
217 DNA samples were stored at -20°C.

**218 Verticillium race determination by specific PCR assay**

219 Race-specific determination was performed using the primers Vd\_Ave1\_F1 (5'-  
220 ACTCGCCAGAAGAAGTCCAA- 3') and Vd\_Ave1\_R1 (5'-  
221 CCACAACAGGGAGACAGGTT- 3'). The primers were designed by Primer3 software  
222 (Koressaar and Remm, 2007; Untergasser *et al.*, 2012). The *Ave1* sequence obtained from *V.*  
223 *dahliae* strain St14.01 (accession no. JQ625341) was used as template. In this experiment,  
224 strains that lack *Ave1* could belong to race 2. The strains VdLs16 race 1 and VdLs17 race 2  
225 DNA were used as controls. Primers targeting the ITS region Vd-ITS1-45-F and Vd-ITS2-  
226 379-R (Bressan *et al.*, 2016) were used as a positive control to guarantee the presence of the  
227 DNA samples. End-point PCR was performed in a 25 µL reaction volume: 50 ng of fungal  
228 DNA (pure culture), 0.1 µM of each primer (Vd\_Ave1\_F1 and Vd\_Ave1\_R1) and 12.5 µL of  
229 GoTaq® Green Master Mix (Promega, Madison WI, USA). PCR cycling was achieved using

230 a GeneAmp® PCR System 9700 (Applied Biosystems, Foster City CA, USA) following the  
231 program: 95°C, 2 minutes then 35 cycles of 95°C, 45 seconds; 60°C; 1 minute; 72°C; 30  
232 seconds; and finally 72°C, 7 minutes for final extension. The PCR products, with an expected  
233 amplicon size of 216 bp, were visualized by electrophoresis on 1% agarose gel stained by  
234 ethidium bromide.

### 235 ***V. dahliae* detection on plant samples by PCR assay**

236 *V. dahliae* detection was performed using the primers Vd-ITS1-45-F and Vd-ITS2-379-R  
237 (Bressan *et al.*, 2016). End-point PCR was performed in a 25 µL reaction volume: 50 ng of  
238 plant DNA (stem or straw, non-infected or infected), 0.1 µM of each primer (Vd-ITS1-45-F  
239 and Vd-ITS2-379-R) and 12.5 µL of GoTaq® Green Master Mix (Promega, Madison WI,  
240 USA). PCR cycling was achieved using a GeneAmp® PCR System 9700 (Applied  
241 Biosystems, Foster City CA, USA) following the program: 95°C, 2 minutes then 35 cycles of  
242 95°C, 45 seconds; 60°C; 1 minute; 72°C; 30 seconds; and finally 72°C, 7 minutes for final  
243 extension. The PCR products, with an expected amplicon size of 334 bp, were visualized by  
244 electrophoresis on 1% agarose gel stained by ethidium bromide.

## 245 **Results**

### 246 **Identification of VdLu01, a *V. dahliae* isolate from fiber flax**

247 After one week growing on PDA-agar medium, the strain VdLu01 produced a white colony  
248 (Fig. 1A); an abundant and floccose aerial mycelium was observed. According to  
249 morphological traits described by Inderbitzin *et al.*, (2011), conidiophores were erect and  
250 branched, narrowing towards the apex, hyaline and septate. Phialides were flask-shaped,  
251 arranged in whorls along conidiophores, pointed and carrying ovoid and hyaline terminal  
252 conidia (Fig. 1E). Furthermore, when cultivated in MA-liquid medium for one month,  
253 VdLu01 formed microsclerotia composed of rounded brown-pigmented cells (Fig. 1B and

254 1H) embedded in a mycelial matrix (Fig. 1G). Occasionally, hyphae formed by torulose cells  
255 were attached to a microsclerotium (Fig. 1F). The ITS region specific to *V. dahliae* (Bressan  
256 *et al.*, 2016) was detected on VdLu01 and the lettuce isolates VdLs16 and VdLs17 (Fig. 1C),  
257 whereas *Ave1* sequence was detected neither on VdLu01 nor on VdLs17, thus both could be  
258 assigned to race 2 (Fig. 1D).

### 259 **Pathogen development and symptoms on root**

260 Symptom observations were performed using the strains VdLu01 and VdLs17. In both  
261 infections, first root symptoms triggered rapidly. Lateral roots exhibited dryness and a brown  
262 discoloration on surface was observed (Fig. 2B). Occasionally, these roots were tightly  
263 hanging on the main root by fungal mycelium (Fig. 2D). Additionally, a brown discoloration  
264 of epidermis and vascular tissues in the main root was noticed (Fig. 2F).

265 Time-course tracking of pathogen development by CLSM was undertaken using the GFP-  
266 tagged VdLs17 strain. Two hours after inoculation performed by the root-dipping method, the  
267 entire root was covered by conidia, including the zone of cell differentiation, lateral roots, root  
268 hairs, zone of cell elongation and root tips. Conidia were randomly distributed, isolated or in  
269 heaps and spotted on the root epidermis (Fig. 3C, 3D and 3E). By 2 hours post inoculation  
270 (hpi), germination of conidia was observed; only one germ tube emerged from one end per  
271 cell (Fig. 3A and 3B). One day post inoculation (dpi), hyphae had grown parallel to the  
272 longitudinal axis of the root or not, occasionally developing secondary structures along the  
273 main hyphae (Fig. 3F, 3G and 3H). The growth pattern of most hyphae followed a random  
274 path, but it is likely that the hyphae extended over a maximum area along the root surface  
275 (Fig. 3H). At the same time, some conidia germinated and developed a germ tube; others  
276 remained in a quiescent state on the root epidermis (Fig. 3F). Interestingly, whereas  
277 successful germination of conidia and hyphal development was found on the zone of cell

278 differentiation and lateral roots, the zone of cell division and root tip were free of the  
279 pathogen. By 3 dpi, the pathogen developed from the tip of lateral roots (Fig. 3I) but also, a  
280 large fungal mass extended on the zone of cell differentiation and lateral roots, encompassing  
281 the entire area, sometimes developing in the periphery (Fig. 3J). Consequently, these sections  
282 of roots were covered by the pathogen, causing dryness of lateral roots, collapse of tissues and  
283 cessation of meristematic activity in some cases. These symptoms were in correlation to the  
284 observations performed by the light reflection microscope. By 1 week post inoculation (wpi),  
285 the zone of cell differentiation was entirely colonized by the fungus. Most hyphae were  
286 oriented parallel with the longitudinal axis of the root (Fig. 3K and 3L). Simultaneously, on  
287 some areas of the zone of cell differentiation, each oriented mycelial hyphae developed  
288 several swelling structures similar to appressoria, in contact with the junction of two  
289 epidermal cells (Fig. 4A and 4B). It is likely that these weakly protected areas are the point of  
290 entry of intercellular colonization into the cortical tissues leading to vascular colonization.  
291 However, no cortical intercellular colonization was observed. By 2 wpi, colonization of the  
292 root vascular system by the pathogen was clearly observed (Fig. 4C and 4D): a set of several  
293 hyphae followed the path of the vascular tissues (Fig. 4E and 4F). As in the main root,  
294 vascular colonization occurred in lateral roots. The pathogen was always detected on the basal  
295 area, whereas it was still absent from apical areas of the root. Interestingly, once vascular  
296 colonization was established, no additional pathogen was observed on the root surface (Fig.  
297 4C, 4E and 4G). Cross-sections of the main root at 4 wpi confirmed the pathogen colonization  
298 within the xylem vessels (Fig. 4G, 4H and 4I). Not all vessels were filled by the pathogen  
299 (Fig. 4G, 4H and 4I), and those contaminated were filled with different amounts of hyphae  
300 (Fig. 4H).

### 301 **Pathogen development and symptoms on stem and leaves**

302 In VdLu01 infections, some early symptoms occasionally appear on seedlings or plants with  
303 growth retardation after 1 wpi: apical leaves exhibited chlorosis and an altered morphology  
304 (data not shown). In both infections (VdLu01 or VdLs17), wilting symptoms on leaves started  
305 between three and four wpi (Fig. 5B). Necrosis was displayed first at the leaf tips, which turn  
306 yellow and roll up (Fig. 5A). Over the following weeks, necrosis extended to the whole leaf,  
307 but did not reach or affect the stem, and falling leaves could be observed (Fig. 5A). These  
308 symptoms were always observed first at the base, and then spread to the apex, clearly showing  
309 the growing symptoms to be acropetal (Fig. 5B). However, this growth of symptoms appeared  
310 to be very slow. Furthermore, a brown vascular discoloration was observed within the basal  
311 part of the stem (hypocotyl) at 4 wpi (Fig. 5D).

312 Further CLSM investigations at 4 wpi confirmed extensive pathogen colonization within the  
313 root whereas a weak fluorescent signal was detected within the hypocotyl (Fig. 6A and 6B).  
314 More, neither symptomatic leaves nor apical part of the stem revealed the presence of the  
315 pathogen. Therefore, symptoms, including the brown discoloration and wilting leaves  
316 appeared well in advance of the presence of the pathogen. Nevertheless, growth into vascular  
317 tissues was slow. Between 6 and 8 wpi, observations on the stem were then performed  
318 between the cotyledon and tenth leaf. Longitudinal sectioning of the stem was necessary to  
319 detect the GFP signal; actually, it revealed a high signal around the pith showing the acropetal  
320 growth of pathogen hyphae (Fig. 6H). Nevertheless, the pathogen did not colonize the entire  
321 area around the pith. No hyphal progression was observed toward the leaves. Further  
322 information was obtained by observation of the stem cross sections. Similarly to what was  
323 observed in root, xylem vessels were partially colonized by various quantity of pathogen  
324 hyphae (Fig. 6F and 6G), and several neighboring vessels, or only a single vessel, were  
325 occasionally colonized (Fig. 6C and 6E). Finally at this time, the pathogen could disturb the  
326 hydraulic system but the fiber bundles were not invaded (Fig. 6D and 6E). Symptomatic

327 lower and upper leaves samples were collected and did not exhibit macroscopic differences.  
328 The pathogen invaded vascular tissues of the midrib and veins in lower leaves only (Fig. 6I).  
329 The pathogen did not colonize the entire leaf, only the basal area toward the apical area (Fig.  
330 6J).

### 331 **Observations of Verticillium wilt in field**

332 At the capsule stage, wilted plants were randomly distributed within an area of the plot (Fig.  
333 7A). On the infected plants sampled, the global aspect of infected plants exhibited typical  
334 wilting symptoms, fewer capsules were observed as compared to the non-infected plants (Fig.  
335 7C and 7D). Stems were dried and chlorotic on apical parts, containing small black spots (Fig.  
336 7E). Leaves were rolled up and contained black fungal mycelium (Fig. 7D). On the brittle  
337 straws sampled after retting, reflection microscopy revealed numerous black microsclerotia on  
338 the surface of brittle straws (Fig. 7F). Several dry fungal structures similar to brown-  
339 pigmented torulose cells were observed on the internal parts of the epidermal tissues,  
340 seemingly forming a microsclerotium (Fig. 7G). After retting, the bast fiber bundle was easily  
341 removable from the straw and also, contained numerous black microsclerotia (Fig. 7H).  
342 Closest investigations revealed that microsclerotia were embedded inside the bast fiber bundle  
343 (Fig. 7I), thus potentially involved in brittleness of infected fibers. PCR amplification  
344 confirmed presence of *V. dahliae* both on infected plants and brittle straws (Fig. 7B).

### 345 **Discussion**

346 Here, we provide the first report of how the pathogen *V. dahliae* develops in fiber flax roots  
347 and above-ground parts using VdLs17 (isolated from lettuce) and previously transformed with  
348 the GFP gene. The strain VdLs17 belongs to race 2 (Vallad *et al.*, 2006) and lacks the *AveI*  
349 sequence, as does the strain VdLu01 isolated from fiber flax. Fiber flax exhibits wilting  
350 symptoms after three or four weeks similarly when inoculated by VdLs17 or VdLu01 in both

351 inoculation systems. Therefore, VdLs17 can be considered to be a flax pathogen. Bhat and  
352 Subbarao (1999) have reported cross-pathogenicity of isolates from specific crops on a set of  
353 host plants e.g. bell pepper, cabbage, cauliflower, cotton, eggplant and mint isolates. In  
354 addition, *Nicotiana benthamina* exhibits wilting symptoms after 12 days when inoculated by  
355 the lettuce strain VdLs17 (Klosterman *et al.*, 2011). These observations support the idea that  
356 *V. dahliae* rapidly adapts to new niche hosts.

357 Although microsclerotia are the primary source of inoculum in infested soils, conidia  
358 suspension were preferentially selected to initiate infection because conidia are quite uniform,  
359 making them easier to prepare and quantify relative to microsclerotia (Vallad *et al.*, 2008). In  
360 our report, 3 different main steps are distinguishable: development on the root epidermis  
361 broadly asymptomatic, colonization within the root xylems then, those of the stem and leaves  
362 leading to symptoms. During the first steps of infection, conidia germinate probably due to  
363 root exudates that overcome fungistasis (Schreiber and Green, 1963), giving rise to mycelia  
364 hyphae that extend over a maximum area of between 2 hpi and 1 dpi. Subsequently, the  
365 pathogen develops at 3 dpi only on the zone of cell differentiation and lateral roots, causing  
366 dryness, brown discoloration and collapse of tissues as a consequence of massive surface  
367 colonization. This fungal mass tends to organize itself along the longitudinal axis of the  
368 epidermal cells at 7 days. In contrast, Zhang *et al.* (2012) observed pathogen development on  
369 the meristematic and the elongation zones of cotton roots. Nevertheless, colonization of  
370 lateral roots leading to a successful infection was reported on *Arabidopsis* and lettuce (Vallad  
371 and Subbarao, 2008; Zhao *et al.*, 2014). Zhao *et al.* (2014) reported in *Arabidopsis* that  
372 despite massive hyphae encompassing the root surface, only a few hyphae successfully  
373 invaded the root internal tissues. The same observation was previously reported for cotton  
374 roots (Zhang *et al.* 2012). Observations at 7 dpi revealed several swelling structures similar to  
375 appressoria developed along mycelia hyphae on the root surface. The pathogen tends to

376 colonize inner tissues through epidermal cell junctions. These observations confirm the  
377 presence of appressoria as structures of penetration. However, pathogen colonization did not  
378 spread onto the zone of cell elongation and root tip after 1 dpi, contrary to reports on spinach,  
379 cotton and lettuce (Vallad and Subbarao, 2008; Zhang *et al.* 2012; Maruthachalam *et al.*  
380 2013), suggesting that these zones are particularly distant from the infection in this study.  
381 Indeed, the zone of cell elongation is generally considered to be a major site for the exudation  
382 of secondary metabolites (McDougall and Rovira, 1970). A previous study notes that MAMPs  
383 (Microbe-associated molecular patterns) such as the flagellar peptide (Flg22) and  
384 peptidoglycan (PGN) trigger a defense response in the epidermal layer of the cell elongation  
385 zone in *Arabidopsis* (Millet *et al.*, 2010). Border cells, cells that are separated from the root  
386 tip of higher plants and produce metabolites in the rhizosphere (Hawes *et al.*, 2000), protect  
387 the pea root meristem when infected by *Nectria haematococca* (Gunawardena and Hawes,  
388 2002; Gunawardena *et al.*, 2005). Border-like cells of *Arabidopsis* and flax respond to Flg22  
389 and PGN by triggering an oxidative burst, the expression of defense-related genes and cell  
390 wall redistribution of extensins (Plancot *et al.*, 2013).

391 Vascular colonization into root was observed for the first time at 2 wpi in the main root as  
392 well as in lateral roots but the colonization of xylems was incomplete. In susceptible lettuce  
393 taproot, restricted advancement of mycelia through xylem vessels has also been observed  
394 (Vallad and Subbarao, 2008). This is in contrast to observations in spinach, where all xylem  
395 vessels are heavily colonized (Maruthachalam *et al.* 2013). The pathogen remains in roots  
396 during the following two weeks. It was suggested that wilt pathogens exploit this niche to  
397 avoid competition with other microbes (McCully, 2001). The xylem is a nutritionally poor  
398 environment; nevertheless, analysis of whole genome sequences reveals that the *V. dahliae*  
399 genome is enriched in genes encoding CWDEs (Cell wall degrading enzymes), which are  
400 implicated in cell walls degradation to release sugar as a source of nutrition (Klosterman *et*

401 *al.*, 2011). Once entering xylem vessels, *V. dahliae* is faced with a set plant defense reactions  
402 combining tyloses, pectin gels and gums, phenolic compounds and inorganic sulfur (Yadeta  
403 and Thomma, 2013).

404 In our study, common wilting symptoms emerged between three and four weeks after *V.*  
405 *dahliae* inoculation and grew acropetally. Wilting symptoms are also a consequence of  
406 *Fusarium oxysporum* f.sp. *lini* infection (Kroes *et al.*, 1999); reports in the field show that  
407 Fusarium wilt can occur at any time of the growing season, and symptoms generally start on  
408 upper leaves (Rashid, 2003). Therefore, basipetal development of foliar symptoms is a feature  
409 of Fusarium wilt whereas acropetal symptoms development is one of Verticillium wilt. Based  
410 on this difference, symptom diagnosis in the field could distinguish Fusarium wilt from  
411 Verticillium wilt. In addition, as recommended for an early diagnostic on lettuce (Vallad *et*  
412 *al.*, 2006), the onset of the root vascular brown discoloration in advance of the pathogen could  
413 be an early diagnostic on fiber flax as well. Because of a lack of a reliable diagnosis for  
414 Verticillium wilt in early steps of cultivation, combining PCR with symptomatology of plant  
415 samples could be an efficient approach to detecting cases of Verticillium wilt in the field. In  
416 recent years, real-time PCR has gained in popularity for Verticillium wilt detection and  
417 quantification in seeds (Karajeh *et al.*, 2006; Maruthachalam *et al.* 2013), environmental  
418 samples (Banno *et al.*, 2011; Bilodeau *et al.*, 2012) and symptomatic plants from the field  
419 (Mercado-Blanco *et al.*, 2003; Atallah *et al.*, 2007) because it is accurate and sensitive.  
420 Necrotic leaves at four weeks did not display the presence of the pathogen; it takes two  
421 additional weeks to detect hyphae within the midrib and veins of leaves. On infected lettuce,  
422 Vallad and Subbarao (2008) reported the presence of hyphae moving through the midrib and  
423 veins within chlorotic regions of leaves occurring after symptoms appear. Actually, there is no  
424 consensus about the physiological and biochemical basis of Verticillium wilt symptoms.  
425 Several studies demonstrated *V. dahliae* secretome activity that is detrimental to plant tissues

426 such as Nep or NEP protein elicitors. Recombinant VdNEP causes symptoms on tobacco and  
427 cotton, although recombinant NLP1 and NLP2 cause symptoms on tobacco only the NLP1  
428 knockout mutant stops symptoms on tobacco (Wang *et al.*, 2004; Wang *et al.*, 2012;  
429 Santhanam *et al.*, 2013). Other studies note the symptoms to be an unfortunate secondary  
430 consequence of the host response; among them, the TMP1 protein, a defense response to *V.*  
431 *dahliae*, contributes to one aspect of symptom development, namely water restriction and  
432 wilting of the host (Robb *et al.*, 1983; 1989).

433 Finally, between six and eight wpi, the pathogen was sequestered within stem xylem vessels.  
434 However, pathogen progression had yet not reached the bast fiber bundle. Generally, fiber  
435 flax cultivation requires at least 120 days obtaining long fibers, followed by a retting process  
436 to dissociate the fibers from the other parts of the stem. Damage caused by *Verticillium* wilt  
437 to fiber flax differs from other crops because the inner tissues (bast fiber bundles) are affected  
438 and therefore unmarketable. It could be suggested that fiber deterioration can occur later, once  
439 the plant is no longer capable of protecting itself, i.e., during retting. Our report in field  
440 revealed that *V. dahliae* has reached the fiber after retting, numerous microsclerotia were  
441 embedded inside the bast fiber bundle, consequently contribute potentially to weakening of  
442 fiber. Cellulose is the major compound of fiber's secondary cell wall, ranging from 65 to 80%  
443 of dry weight at maturity. Cellulose is encompassed into a hemicellulose and pectin matrix  
444 that ensures cohesion (Morvan *et al.*, 1989; Focher, 1992; Baley *et al.*, 2002). Analysis of the  
445 *V. dahliae* genome shows genes encoding CWDEs, including polysaccharide lyases,  
446 glycoside hydrolases, carbohydrate binding modules, glycosyl transferases and carbohydrate  
447 esterases. Polysaccharide lyases are well represented in the *V. dahliae* genome in comparison  
448 with other Ascomycota; therefore, it is able to cleave different forms of pectin (Klosterman *et*  
449 *al.*, 2011). Accordingly, the process of how and when the fiber is degraded by the pathogen  
450 remains an interesting question.

451 **Acknowledgments**

452 This work was supported by a “Région Haute Normandie” and FERDER grant.

453 Acknowledgements go to Damien Chapman and Magalie Bénard at Primacen platform for

454 their help with CLSM, Terre de lin for supplying fiber flax seeds and Department of Plant

455 Pathology (UC Davis, CA USA) for supplying *V. dahliae* GFP expressing strains VdLs16 and

456 VdLs17.

457

458 **Literature cited**

459

- 460 1. Agrios, G.N. 1997. Plant Pathology. San Diego: Academic Press. 635 pp.
- 461 2. Agrios, G.N. 2005. Plant Pathology. Burlington: Elsevier Academic Press.
- 462 3. Atallah, Z.K., Bae, J., Jansky, S.H., Rouse, D.I., and Stevenson, W.R. 2007. Multiplex  
463 Real-Time Quantitative PCR to Detect and Quantify *Verticillium dahliae* Colonization  
464 in Potato Lines that Differ in Response to Verticillium Wilt. *Phytopathology* 97:865-  
465 72.
- 466 4. Baley, C. 2002. Analysis of flax fibres tensile behaviour and analysis of the tensile  
467 stiffness increase. *Composites Part A*. 33:939-948.
- 468 5. Banno, S., Saito, H., Sakai, H., Urushibara, T., Ikeda, K., Kabe, .T, Kemmochi, I., and  
469 Fujimura, M. 2011. Quantitative nested real-time PCR detection of *Verticillium*  
470 *longisporum* and *V. dahliae* in the soil of cabbage fields. *J. Gen. Plant Pathol.* 77:282-  
471 291.
- 472 6. Bejarano-Alcazar, J., Termorshuizen, A.J., and Jimenez-Diaz, R.M. 1999. Single-site  
473 root inoculations on eggplant with microsclerotia of *Verticillium dahliae*.  
474 *Phytoparasitica* 27:279-289.
- 475 7. Bhat, R. G., and Subbarao, K. V. 1999. Host range specificity in *Verticillium dahliae*.  
476 *Phytopathology* 89:1999-1219.
- 477 8. Bilodeau, G.J., Koike, S.T., Uribe, P., and Martin, F.N. 2012. Development of an  
478 assay for rapid detection and quantification of *Verticillium dahliae* in soil.  
479 *Phytopathology* 102:331-343.
- 480 9. Bressan, M., Blum, A., Castel, L., Trinsoutrot-Gattin, I., Laval, K., and Gangneux, C.  
481 2016. Assessment of *Verticillium* flax inoculum in agroecosystem soils using real-  
482 time PCR assay. *Appl. Soil Ecol.* 108:176-186.

- 483 10. de Jonge, R., van Esse, H. P., Maruthachalam, K., Bolton, M. D., Santhanam, P.,  
484 Saber, M. K., Zhang, Z., Usami, T., Lievens, B., and Subbarao, K. V. 2012. Tomato  
485 immune receptor *Ve1* recognizes effector of multiple fungal pathogens uncovered by  
486 genome and RNA sequencing. Proc. Natl. Acad. Sci. U.S.A. 109:5110-5115.
- 487 11. Devay, J.E., Forrester, L.L., Garber, R.H., and Butterfield, E.J. 1974. Characteristics  
488 and concentration of propagules of *Verticillium dahliae* in air-dried field soils in  
489 relation to prevalence of Verticillium wilt in cotton. Phytopathology 64:22-29.
- 490 12. Diwan, N., Fluhr, R., Eshed, Y., Zamir, D., and Tanksley, S.D. 1999. Mapping of *Ve*  
491 in tomato: a gene conferring resistance to the broad-spectrum pathogen, *Verticillium*  
492 *dahliae* race 1. Theor. Appl. Genet. 98: 315-319.
- 493 13. Eastburn, D.M., and Chang, R.J. 1994. *Verticillium dahliae*: a causal agent of root  
494 discoloration of horseradish in Illinois. Plant Dis. 78:496-98.
- 495 14. Fitt, D.D.L., Bauers, F., Burhenne, S., and Paul, V.H. 1992. Occurrence of  
496 *Verticillium dahliae* on linseed (*Linum usitatissimum*) in the UK and Germany. Plant  
497 Pathol. 41:86-90.
- 498 15. Fitzell, R., Evans, G., and Fahy, P.C. 1980. Studies on the colonization of plant roots  
499 by *Verticillium dahliae* Klebahn with use of immunofluorescent staining. Aust. J. Bot.  
500 28:357-368.
- 501 16. Focher, B., Marzetti, A., and Sharma, H.S.S. 1992. Changes in the structure and  
502 properties of flax during processing. in Biology and Processing of Flax, H. S. S.  
503 Sharma and C. F. van Sumere, Eds., pp. 329-342, M. Publications, Belfast, Northern  
504 Ireland.
- 505 17. Fradin, E. F., and Thomma, B. P. H. J. 2006. Physiology and molecular aspects of  
506 Verticillium wilt diseases caused by *V. dahliae* and *V. alboatrum*. Mol. Plant Pathol.  
507 7:71-86.

- 508 18. Fradin, E.F., Zhang, Z., Ayala, J.C.J., Castroverde, C.D.M., Nazar, R.N., Robb, J.,  
509 Liu, C.M., and Thomma, B.P.H.J. 2009. Genetic dissection of *Verticillium* wilt  
510 resistance mediated by tomato Ve1. *Plant Physiol.* 150: 320-332.
- 511 19. Gerik, J.S., and Huisman, O.C. 1988. Study of field-grown cotton roots infected with  
512 *Verticillium dahliae* using an immunoenzymatic staining technique. *Phytopathology*  
513 78:1174-1178.
- 514 20. Grogan, R., Ioannou, N., Schneider, R., Sall, M., and Kimble, K. 1979. *Verticillium*  
515 wilt on resistant tomato cultivars in California: virulence of isolates from plants and  
516 soil and relationship of inoculum density to disease incidence. *Phytopathology*  
517 69:1176-1180.
- 518 21. Gunawardena, U., and Hawes M.C. 2002. Role of border cells in localized root  
519 infection by pathogenic fungi. *Mol. Plant Microbe Interac.* 15: 1128-1136.
- 520 22. Gunawardena, U., Rodriguez, M., Straney, D., Romeo, J.T., VanEtten, H.D., and  
521 Hawes, M.C. 2005. Tissue-specific localization of pea root infection by *Nectria*  
522 *haematococca*. Mechanisms and consequences. *Plant Physiol.* 137:1363-1374.
- 523 23. Hawes, M.C., Gunawardena, U., Miyasaka, S., and Zhao, X. 2000. The role of root  
524 border cells in plant defense. *Trends Plant Sci.* 5: 128-133.
- 525 24. Hoagland, D.R. and Arnon, D.I. 1950. The Water-Culture Method for Growing Plants  
526 without Soil. California Agricultural Experiment Station Circular. 347, 1-32.
- 527 25. Hoffmann, G.M., and Rondonanski, W. 1959. Eine Verticilliose des Leins (*Linum*  
528 *usitatissimum* L.) in Deutschland. *Nachrichtenblatt für den Deutschen*  
529 *Pflanzenschutzdienst*, Berlin 13, 91-9.
- 530 26. Inderbitzin, P., and Subbarao, K.V. 2014. *Verticillium* Systematics and Evolution:  
531 How Confusion Impedes *Verticillium* Wilt Management and How to Resolve It.  
532 *Phytopathology* 104:564-74.

- 533 27. Inderbitzin, P., Bostock, R.M., Davis, R.M., Usami, T., Platt, H.W., and Subbarao,  
534 K.V. 2011. Phylogenetics and Taxonomy of the Fungal Vascular Wilt Pathogen  
535 *Verticillium*, with the Descriptions of Five New Species PLoS One 6:e28341.
- 536 28. Karajeh, M.R. 2006. Seed transmission of *Verticillium dahliae* in olive as detected by  
537 a highly sensitive nested PCR-based assay. Phytopathol. Mediterr. 45:15-23.
- 538 29. Kawchuk, L.M., Hachey, J., Lynch, D.R., Kulcsar, F., van Rooijen, G., Waterer, D.R.,  
539 Robertson, A., Kokko, E., Byers, R., Howard, B.J., Fischer, R., and Prüfer, D. 2001.  
540 Tomato *Ve* disease resistance genes encode cell surface-like receptors. Proc. Natl.  
541 Acad. Sci. U.S.A. 98: 6511-6515.
- 542 30. Klosterman, S. J., Subbarao, K. V., Kang, S., Veronese, P., Gold, S. E., Thomma, B.  
543 P. H. J., Chen, Z., Henrissat, B., Lee, Y.-H., Park, J., Garcia-Pedrajas, M. D., Barbara,  
544 D. J., Anchieta, A., de Jonge, R., Santhanam, P., Maruthachalam, K., Atallah, Z.,  
545 Amyotte, S. G., Paz, Z., Inderbitzin, P., Hayes, R. J., Heiman, D. I., Young, S., Zeng,  
546 Q., Engels, R., Galagan, J., Cuomo, C. A., Dobinson, K. F., and Ma, L.-J. 2011.  
547 Comparative genomics yields insights into niche adaptation of plant vascular wilt  
548 pathogens. PLoS Pathol. 7:e1002137.
- 549 31. Klosterman, S.J., Atallah, Z.K., Vallad, G.E., and Subbarao, K.V. 2009. Diversity  
550 pathogenicity and management of *Verticillium* species. Annu. Rev. Phytopathol. 47:  
551 39–61.
- 552 32. Koressaar, T., and Remm, M. 2007. Enhancements and modifications of primer design  
553 program Primer3. Bioinformatics 23:1289-91.
- 554 33. Krikun, J., and Bernier, C.C. 1990. Morphology of microsclerotia of *Verticillium*  
555 *dahliae* in roots of gramineous plants. Can. J. Plant Pathol. 12:439-441.

- 556 34. Kroes, G.M.L.W., Loffler, H.J.M., Parlevliet, J.E., Keizer, L.C.P., and Lange, W.  
557 1999. Interactions of *Fusarium oxysporum* f.sp. *lini*, the flax wilt pathogen, with flax  
558 and linseed. *Plant Path.* 48:491–498.
- 559 35. Marchal, M.E. 1940. Observations et recherches effectuées à la station de  
560 phytopathologie de l'état pendant l'année 1939. *Bulletin de l'institut Agronomique de*  
561 *Gembloux* 9 :1-15.
- 562 36. Maruthachalam, K., Klosterman, S.J., Anchieta, A., Mou, B. and Subbarao, K.V.  
563 2013. Colonization of spinach by *Verticillium dahliae* and effects of pathogen  
564 localization on the efficacy of seed treatments. *Phytopathology*.103:268–280.
- 565 37. McCully, M.E. 2001. Niches for bacterial endophytes in crop plants: a plant biologist's  
566 view. *Funct. Plant Biol.* 28:983–990.
- 567 38. McDougall, B.M., and Rovira, A.D. 1970. Sites of exudation of 14 C-labelled  
568 compounds from wheat roots. *New Phytol.* 69: 999–1003.
- 569 39. Mercado-Blanco, J., Collado-Romero, M., Parrilla-Araujo, S., Rodríguez-Jurado, D.,  
570 and Jiménez-Díaz, R.M. 2003. Quantitative monitoring of colonization of olive  
571 genotypes by *Verticillium dahliae* pathotypes with real-time polymerase chain  
572 reaction. *Physiol. Mol. Plant Pathol.* 63:91.
- 573 40. Millet, Y.A., Danna, C.H., Clay, N.K., Songnuan, W., Simon, M.D., Werck-Reichhart,  
574 D., and Ausubel, F.M. 2010. Innate Immune Responses Activated in Arabidopsis  
575 Roots by Microbe-Associated Molecular Patterns. *The Plant Cell* 22: 973-990.
- 576 41. Morvan, C., Abdul-Hafez, A., Morvan, O., Jauneau, A., and Demarty, M. 1989.  
577 Physicochemical and biochemical studies of polysaccharides solubilized from under-  
578 retted flax. *Plant Physiol. Biochem.* 27: 451-459.
- 579 42. Pegg, G., and Brady, B. 2002. *Verticillium* Wilts. CAB International. Oxford.

- 580 43. Plancot, B., Santaella, C., Jaber, R., Kiefer-Meyer, M.C., and Follet-Gueye, M-L.  
581 2013. Deciphering the responses of root border-like cells of *Arabidopsis* and flax to  
582 pathogen-derived elicitors. *Plant physiol.* 163: 1584–1597.
- 583 44. Rashid, K.Y. 2003. Principal diseases of flax. In: Muir A, Westcott N (eds) *Flax, the*  
584 *genus Linum*. Taylor & Francis, London, UK. pp 102–133.
- 585 45. Rick, C.M., Martin, F.M., and Gentile, A. 1959. Linkage of *Verticillium* resistance  
586 (*Ve*). *Tomato Genet. Coop.* 9:44.
- 587 46. Robb, E.J., Powell, D.A., and Street P.F.S. 1989. Vascular coating: a barrier to  
588 colonization by the pathogen in *Verticillium* wilt of tomato. *Can. J. Bot.* 67:600–607.
- 589 47. Robb, E.J., Street, P.F.S., and Busch, L.V. 1983. Basic fuchsin: a vascular dye in  
590 studies of *Verticillium*-infected chrysanthemum and tomato. *Can. J. Bot.* 61:3355–  
591 3365.
- 592 48. Santhanam, P., van Esse, H.P., Albert, I., Faino, L., Nürnberger, T., and Thomma,  
593 B.P. 2013. Evidence for functional diversification within a fungal NEP1-like protein  
594 family. *Mol. Plant Microbe Interact.* 26:278-286.
- 595 49. Schaible, L., Cannon, O. S., and Waddoups, V. 1951. Inheritance of resistance to  
596 *Verticillium* wilt in a tomato cross. *Phytopathology* 41:986-990.
- 597 50. Schreiber, L.R., and Green, R.J. 1963. Effect of root exudates on germination of  
598 conidia and microsclerotia of *Verticillium alboatrum* inhibited by the soil fungistatic  
599 principle. *Phytopathology* 53:260-264.
- 600 51. Untergasser, A., Cutcutache, I., Koressaar, T., Ye, J., Faircloth, B.C., Remm, M., and  
601 Rozen, S.G. 2012. Primer3 - new capabilities and interfaces. *Nucleic Acids Res.*  
602 40:e115.

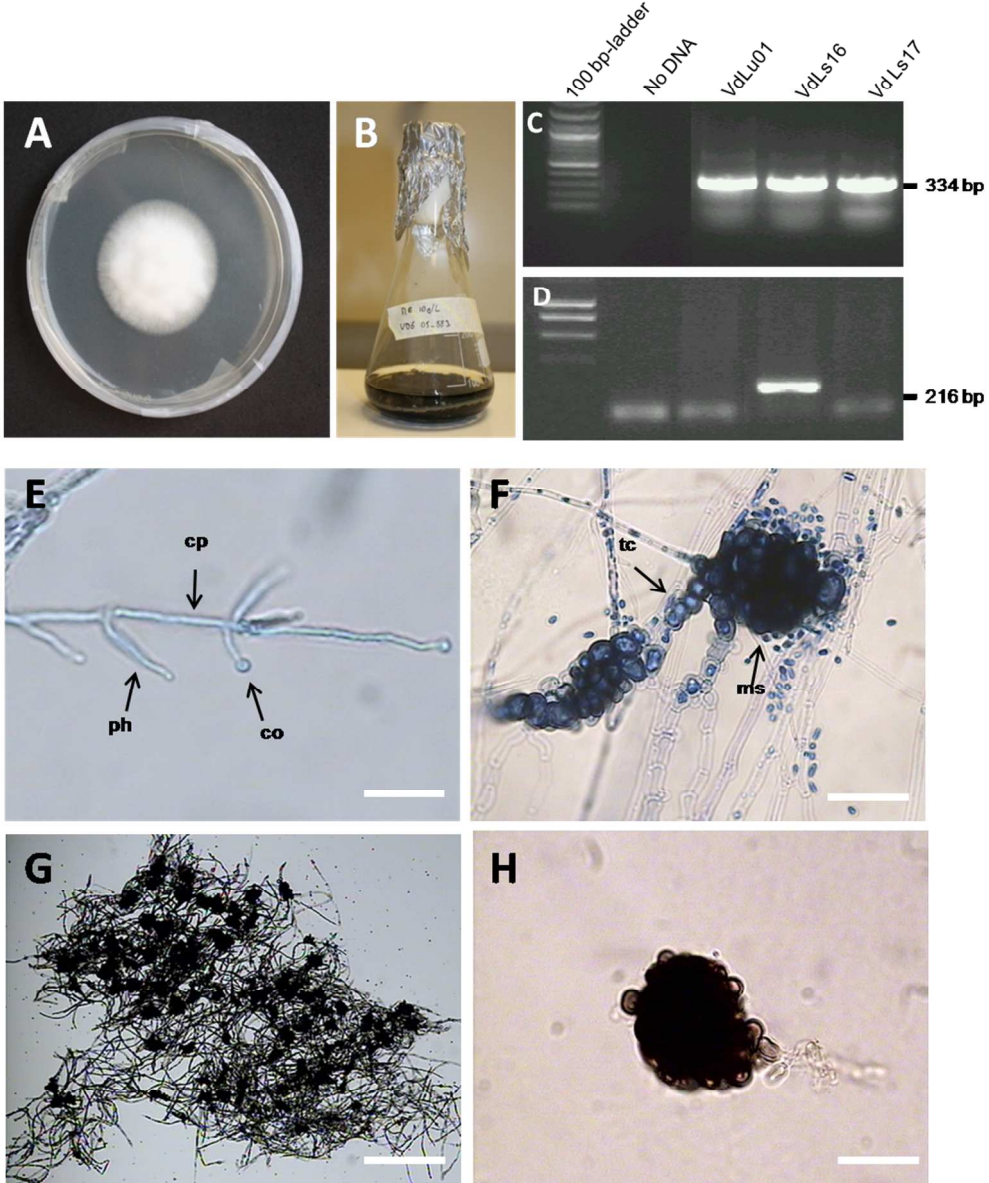
- 603 52. Valade, R., Cast, D., and Bert, F., 2015. Verticilliose du lin fibre, la prévention  
604 comme seule arme. Perspectives agricoles (ed. et Publications agricoles françaises).  
605 424 : 30-32.
- 606 53. Vallad, G. E., Qin, Q.-M., Grube, R., Hayes, R. J., and Subbarao, K. V. 2006.  
607 Characterization of race-specific interactions among isolates of *Verticillium dahliae*  
608 pathogenic on lettuce. Phytopathology 96:1380-1387.
- 609 54. Vallad, G.E., and Subbarao, K.V. 2008. Colonization of Resistant and Susceptible  
610 Lettuce Cultivars by a Green Fluorescent Protein-Tagged Isolate of *Verticillium*  
611 *dahliae*. Phytopathology 98:871-885.
- 612 55. van Sumere, C. 1992. Retting of flax with special reference to enzyme-retting. In:  
613 Sharma,H. and C. Van Sumere (eds.), The Biology and Processing of Flax. M  
614 Publications, Belfast, Northern Ireland, pp: 157-198.
- 615 56. Wang, B., Yang, X., Zeng, H., Liu, H., Zhou T., Guo, L., and Qiu, D. 2012. The  
616 purification and characterization of a novel hypersensitive-like response-inducing  
617 elicitor from *Verticillium dahliae* that induces resistance responses in tobacco. Appl.  
618 Microbiol. Biotechnol. 93:191-201.
- 619 57. Wang, J., Cai, Y., Gou, J., Mao, Y., Xu, Y., Jiang, W., and Chen, X. 2004. VdNEP, an  
620 Elicitor from *Verticillium dahliae*, Induces Cotton Plant Wilting. Appl. Environ.  
621 Microb. 70:4989-4995.
- 622 58. Wilhelm, S. 1955. Longevity of the Verticillium wilt fungus in the laboratory and  
623 field. Phytopathology 45:180-181.
- 624 59. Yadeta, K.A., and Thomma, B.P.H.J. 2013. The xylem as battleground for plant hosts  
625 and vascular wilt pathogens. Front Plant Sci. 4:97.

- 626 60. Zelko, I., Lux, A., Sterckeman, T., Martinka, M., Kollárová, K., and Lišková, D. 2012.  
627 An easy method for cutting and fluorescent staining of thin roots. *Ann. Bot.* 110:475–  
628 478.
- 629 61. Zhang, W., Jiang, T., Cui ,X., Qi, F., and Jian, G. 2012b. Colonization in cotton plants  
630 by a green fluorescent protein labelled strain of *Verticillium dahliae*. *Eur. J. Plant*  
631 *Pathol.* 135: 867-876.
- 632 62. Zhao, P., Zhao, Y., Jin, Y., Zhang, T., and Guo, H. 2014. Colonization process of  
633 *Arabidopsis thaliana* roots by a green fluorescent protein-tagged isolate of  
634 *Verticillium dahliae*. *Protein Cell.* 5: 94-98.

#### 635 **Recommended internet resources**

- 636 Chambre régionale d'agriculture de Normandie : Le lin en Normandie. <http://www.chambre->  
637 [agriculture-normandie.fr/panorama-lin-normandie/](http://www.chambre-agriculture-normandie.fr/panorama-lin-normandie/) (accessed 2017.11.07).
- 638 Arvalis institut du végétal : Fiche accident, la verticilliose sur lin fibre.  
639 <http://www.fiches.arvalis->  
640 [infos.fr/fiche\\_accident/fiches\\_accidents.php?mode=fa&type\\_cul=10&type\\_acc=4&id\\_acc=3](http://www.fiches.arvalis-infos.fr/fiche_accident/fiches_accidents.php?mode=fa&type_cul=10&type_acc=4&id_acc=3)  
641 81 (accessed 2017.11.07).

Plant Disease "First Look" paper • <http://dx.doi.org/10.1094/PDIS-01-18-0139-RE> • posted 05/23/2018  
This paper has been peer reviewed and accepted for publication but has not yet been copyedited or proofread. The final published version may differ.



1  
2

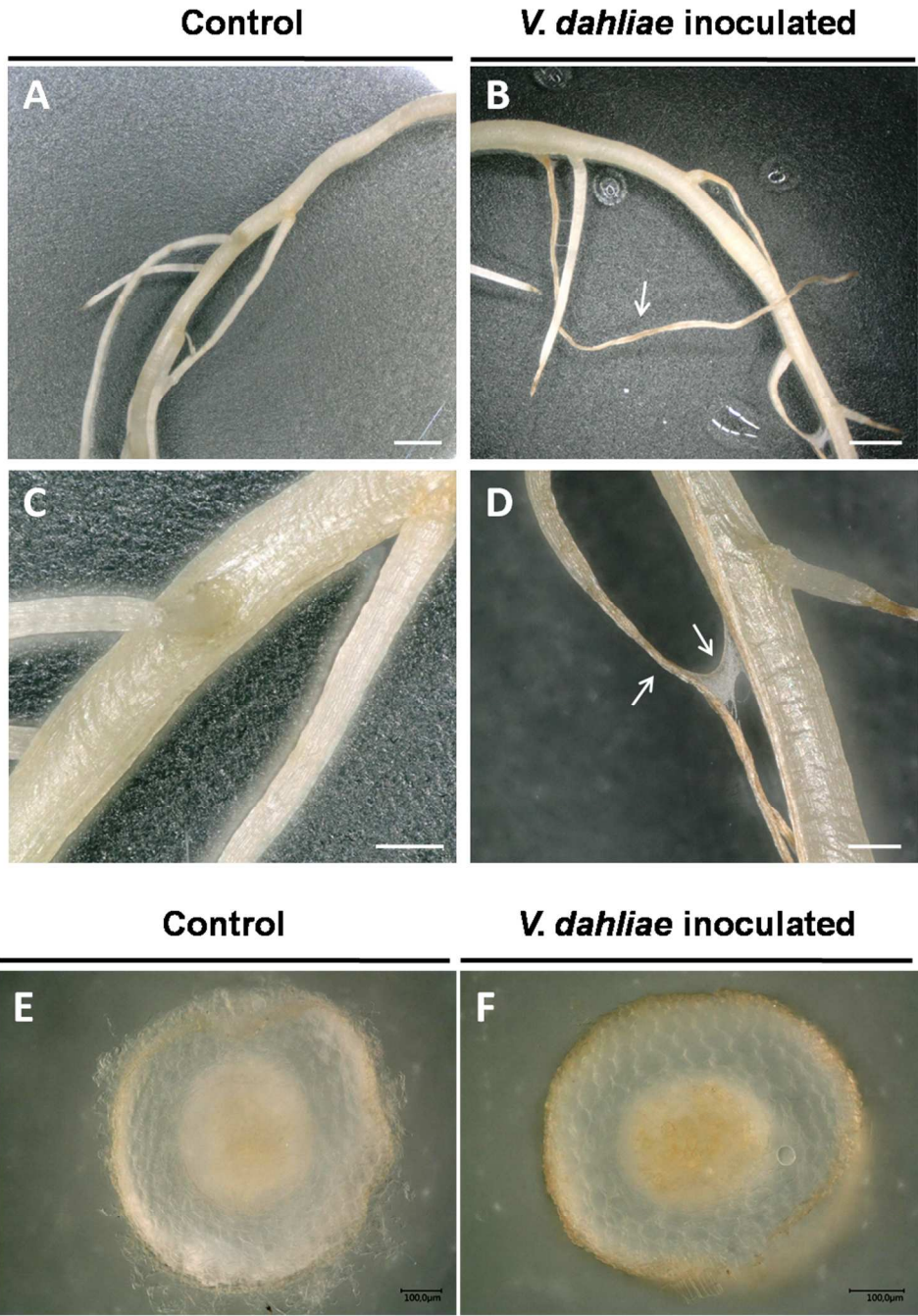
3 **Fig. 1.** Identification of VdLu01, a *V. dahliae* strain isolated on fiber flax  
4 straw. Morphological (A and B, E to H) and molecular (C and D) traits.  
5 Macroscopic aspect of VdLu01 after growing one week on PDA-agar medium  
6 (A) and one month on MA-liquid medium (B). PCR amplification using  
7 primers targeting ITS specific regions of *V. dahliae* (C) or *Ave1* (D) on *V.*  
8 *dahliae* strains VdLu01, VdLs16 and VdLs17. Expected amplicon size 334 bp  
9 (C) or 216 bp (D). Microscopic observation of hyphal structure: apex of a  
10 conidiophore (E), torulose cells surrounding a microsclerotium (F) blue  
11 lactophenol staining; heap of microsclerotia (G) and isolated microsclerotium  
12 (H). co= conidium, cp= conidiophore, ph= phialide, ms= microsclerotia, tc=  
13 torulose cell. Bars= 20  $\mu\text{m}$  (E), 40  $\mu\text{m}$  (F and H) and 200  $\mu\text{m}$  (G).

14

15

16

Plant Disease "First Look" paper • <http://dx.doi.org/10.1094/PDIS-01-18-0139-RE> • posted 05/23/2018  
This paper has been peer reviewed and accepted for publication but has not yet been copyedited or proofread. The final published version may differ.

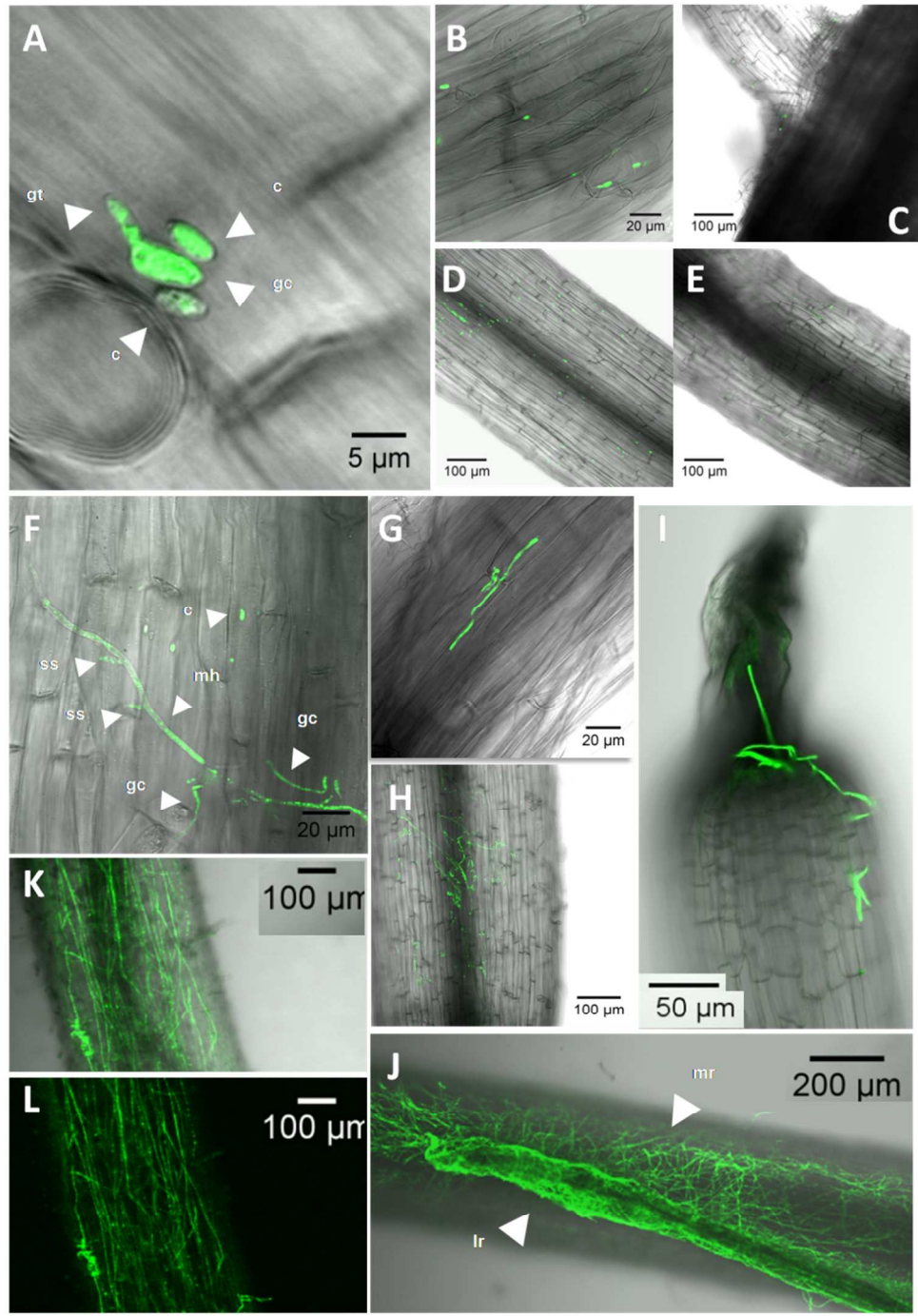


17

18

19 **Fig. 2.** Root symptoms on the zone of cell differentiation and lateral roots  
20 infected by the strains VdLu01 or VdLs17 in (B) and (D), ten dpi. (A) and  
21 (C), roots of control plants for comparison. Bars= 600  $\mu\text{m}$  for (A)(B) or 200  
22  $\mu\text{m}$  for (C)(D). Cross-sections of control (E) and inoculated (F) roots four  
23 wpi. Bars= 100  $\mu\text{m}$ .

Plant Disease "First Look" paper • <http://dx.doi.org/10.1094/PDIS-01-18-0139-RE> • posted 05/23/2018  
This paper has been peer reviewed and accepted for publication but has not yet been copyedited or proofread. The final published version may differ.



24

25

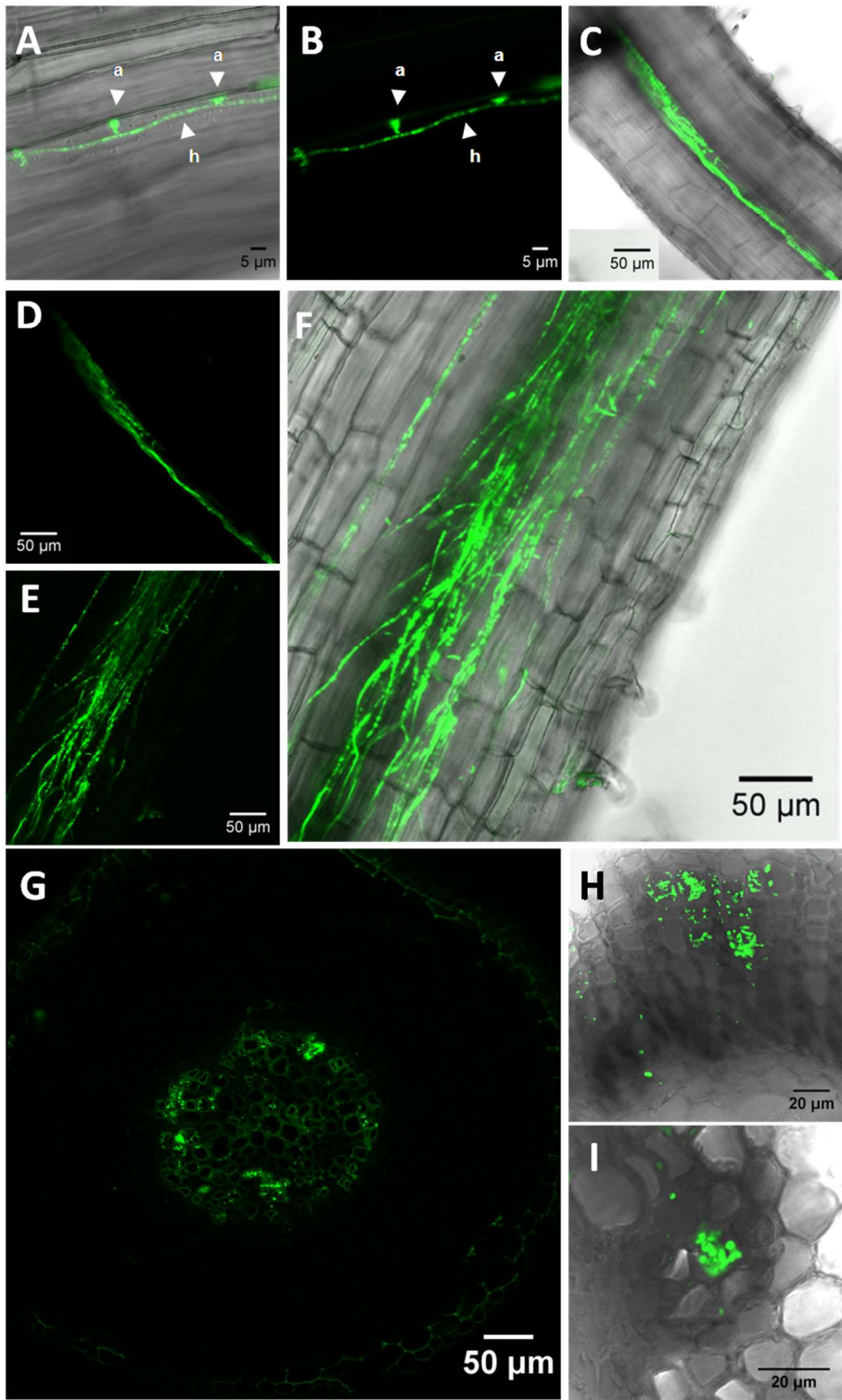
26 **Fig. 3.** Germination of conidia and early steps of hyphae growth of VdLs17  
27 strain on flax roots. Overlay of a bright field image and a fluorescent image.  
28 (A) and (B) Germinated and non germinated conidia on the zone of cell  
29 differentiation, two hpi. (C) and (E) Conidia on the zone of cell differentiation  
30 including lateral root junction (only C), two hpi. (D) Conidia on the zone of  
31 cell elongation, two hpi. (F), (G) and (H) Growth of mycelia hyphae on the  
32 zone of cell differentiation, one dpi (F) and (G); three days dpi (H). (I)  
33 Hyphae caused dryness at the tip of a lateral root, three dpi. (J) Fungal mass  
34 wrapped the zone of cell differentiation including a lateral root, three dpi. (K)  
35 and (L) Growth of mycelia hyphae on the zone of cell differentiation, one  
36 wpi. (L) Only fluorescent image. Co= Conidium, Gc= Germinated conidium  
37 Gt= Germ tube, Mh= Main hypha, Ss= Secondary structure, Lr= Lateral root,  
38 Mr= Main root.

39

40

41

Plant Disease "First Look" paper • <http://dx.doi.org/10.1094/PDIS-01-18-0139-RE> • posted 05/23/2018  
This paper has been peer reviewed and accepted for publication but has not yet been copyedited or proofread. The final published version may differ.



42

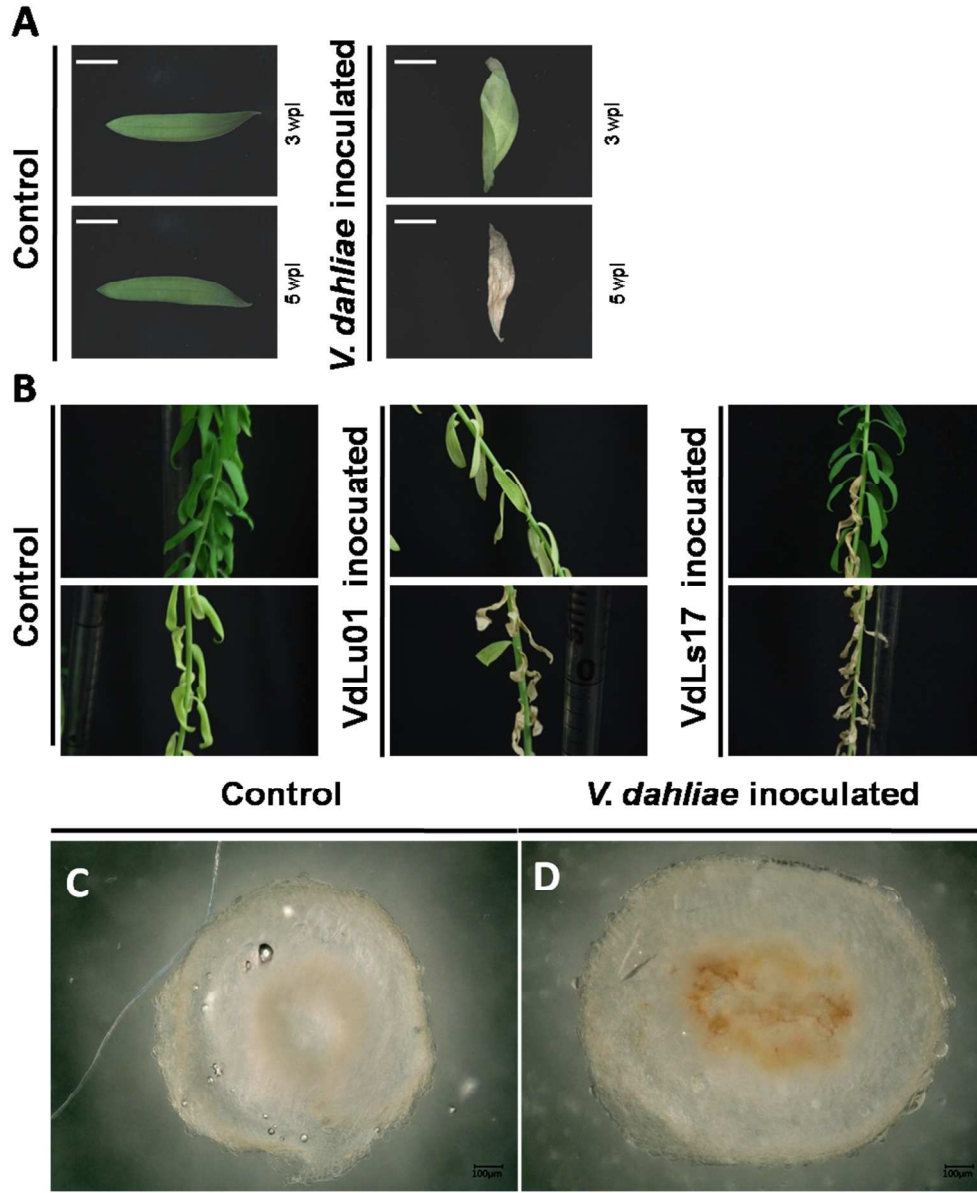
Fig.

43 **4.** Vascular colonization of VdLs17 strain on flax roots. Overlay of a bright  
44 field image and a fluorescent image. (A) and (B) Mycelia hyphae developing  
45 appressoria-like structures on intercellular junction of the zone of cell  
46 differentiation, one wpi. (B) only fluorescent image. (C) to (I) Vascular  
47 colonization of the pathogen in a main root, two wpi (C) to (F), cross-sections  
48 four wpi (G) to (I); (D) (E) and (G) only fluorescent images. (G) Image  
49 stacking (ten images), depth= 60 $\mu$ m . a= Appressorium-like, h= hyphae.

50

51

52



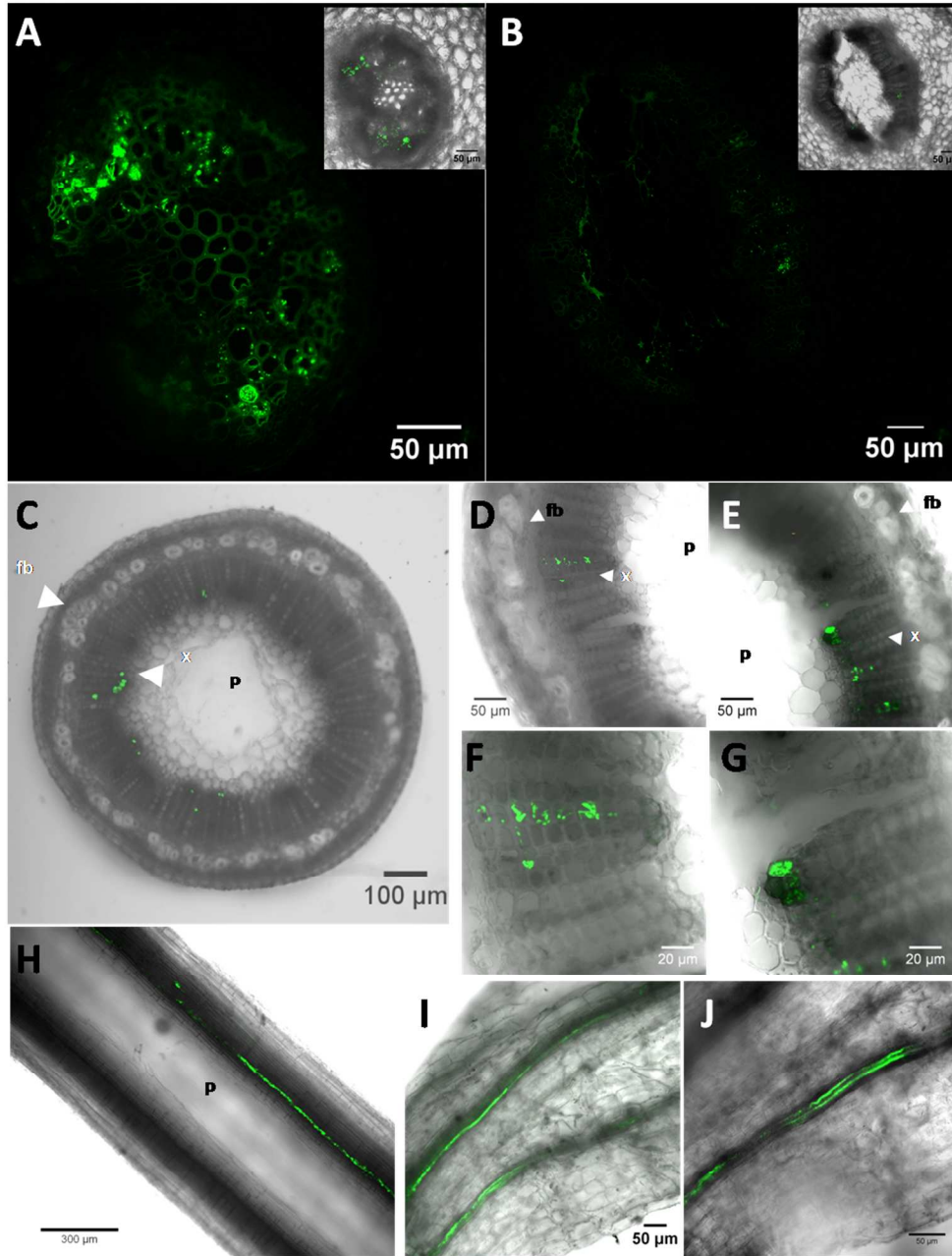
53

54

55 **Fig. 5.** Symptoms of *Verticillium* wilt on stem and leaf of flax. (A) Wilting  
56 symptom on a basal leaf at three and five wpi and control leaf. Bars= 5 mm.  
57 (B) Wilting symptoms at the plant level infected by VdLu01 or VdLs17,  
58 apical and basal level, five wpi and control plant for comparison. (C) Cross-  
59 sections of control (C) and inoculated (D) roots four wpi. Bars= 100  $\mu$ m.

60

61



62

63

64 **Fig. 6.** Vascular colonization of VdLs17 strain within the above-ground parts.  
65 Overlay of a bright field image and a fluorescent image. (A) and (B)  
66 Comparison of pathogen fluorescence within xylem cross-sections of root and  
67 stem (hypocotyl) on the same plant, only fluorescent images, four wpi. (C) to  
68 (J) Between six and eight wpi, (C) to (G) Growth of mycelia hyphae within  
69 stem cross-section. (H) Growth of mycelia hyphae within stem transversal  
70 section. (I) and (J) Growth of mycelia hyphae within basal part of a  
71 symptomatic leaf. Fb= Fiber bundle, P= Pith, X= xylems.

72

73

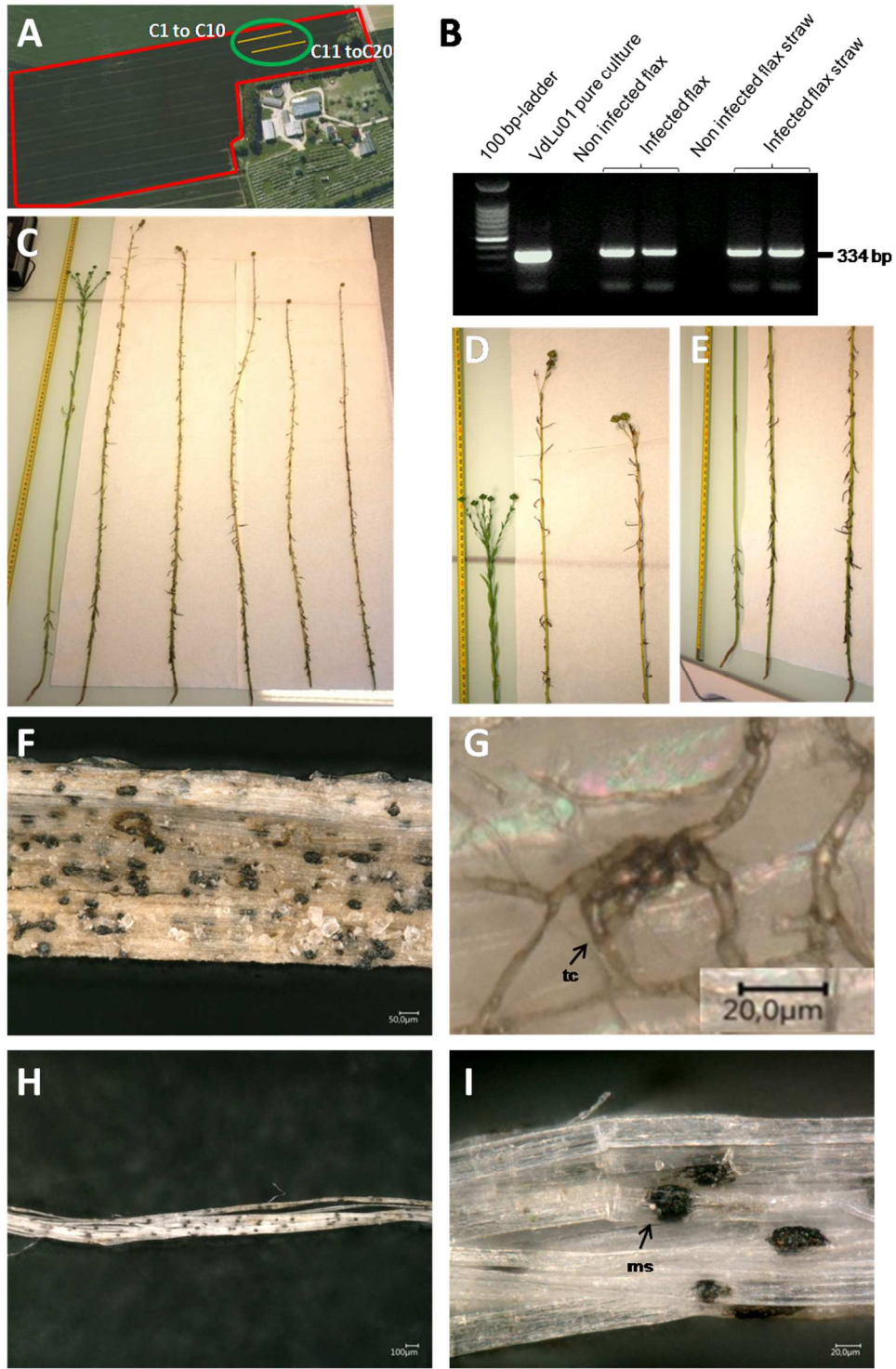
74

75

76

77

Plant Disease "First Look" paper • <http://dx.doi.org/10.1094/PDIS-01-18-0139-RE> • posted 05/23/2018  
This paper has been peer reviewed and accepted for publication but has not yet been copyedited or proofread. The final published version may differ.



79

80 **Fig. 7.** Verticillium wilt caused by *V. dahliae* on flax at the capsule stage and  
81 after retting. (A) Delimitation of the fiber flax plot investigated (red lines),  
82 area where the infectious site was detected (green circle), C1 to C20 (yellow  
83 lines), points where the infected plants were sampled. (B) PCR amplification  
84 using primers targeting ITS specific regions of *V. dahliae* on *V. dahliae* strain  
85 VdLu01, non infected flax, infected flax, non infected flax straw and infected  
86 flax straw. Expected amplicon size 334 bp. (C) to (E) Wilting symptoms on  
87 above-ground parts (non affected plant on left). Close-up view: (D), Apical  
88 parts and (E), basal parts. (F) to (I) Fungal structures of *V. dahliae* on fiber  
89 flax stem after retting. (F) Microsclerotia observed on a straw surface. (G)  
90 Brown-pigmented torulose hyphal cells attached on the internal parts of the  
91 epidermal tissues. (H) Microsclerotia on bast fiber bundles. (I) Close-up view  
92 showing microsclerotia embedded in bast fiber bundle. ms = microsclerotium,  
93 tc = torulose hyphal cells. Bars= 50  $\mu\text{m}$  (F), 20  $\mu\text{m}$  (G) and (I), 100  $\mu\text{m}$  (H).

94

95

96

97